Zeitschrift: IABSE reports of the working commissions = Rapports des commissions de travail AIPC = IVBH Berichte der Arbeitskommissionen

Band: 34 (1981)

Artikel: Inelastic analysis of reinforced concrete shear wall structures: applications and experimental verifications

Autor: Shirai, Nobuaki / Sato, Toshio

DOI: https://doi.org/10.5169/seals-26924

Inelastic Analysis of Reinforced Concrete Shear Wall Structures - Applications and Experimental Verifications -

Analyse inélastique de la structure asismique des refends en béton armé - Ses applications et vérifications expérimentales -

Inelastische Berechnung von erdbebenfesten Stahlbetonwandkonstruktionen - Anwendungen und experimentelle Bestätigung -

NOBUAKI SHIRAI
Assistant

TOSHIO SATO
Professor

Department of Architecture, College of Science and Technology, Nihon University, Tokyo, Japan

SUMMARY

The purpose of this study is to verify the validity and applicability of the material modelling of reinforced concrete proposed by the authors and also to clarify inelastic behavior of reinforced concrete structures.
Numerical examples on tensile bond specimens, reinforced conrete panels and reinforced concrete shear wall-frame structures are given and some numerical results, such as load-deflection curves, internal stress transfer and crack propagation are compared with experimental results.

RÉSUMÉ

Le but de cette étude est de vérifier une validité et une applicabilité de la formule mathématique pour les matériaux de béton armé proposée par les auteurs, ainsi que d'éclaircir les comportements inélastiques de la structure asismique du mur en béton armé. Les exemples numériques sont donnés sur les échantillons d'adhérence à la traction, les panneaux en béton armé, et la structure asismique des refends en béton armé et de l'armature; ensuite, quelques résultats numériques tels que des courbes charge-déflexion, du transfert de contrainte interne et de la propagation des fissures sont comparés avec les résultats expérimentaux.

ZUSAMMENFASSUNG

Der Zweck dieser Forschung besteht darin, die Wirksamkeit und Anwendbarkeiut der von den Autoren vorgeschlagenen Modellierung von Stahlbetonmaterialien zu bestätigen und das inelastische Verhalten von Stahlbetonkonstruktionen zu klären.
Es werden numerische Beispiele für Zughaftproben, Stahlbetonplatten und erdbebenfeste Stahlbetonrahmenkonstruktionen gegeben. Numerische Ergebnisse für Lastverformungskurven, interne Spannungsübertragung, Rissausbreitung usw. werden mit experimentellen Ergebnissen verglichen.

1. INTRODUCTION

The finite element model of reinforced concrete for inelastic effects due to tensile cracking of concrete, nonlinear stress-strain response of concrete and steel, bond between steel and concrete, aggregate interlock between cracked concrete surfaces and dowel action of reinforcing bar was proposed by the authors in the reference[1] in order to investigate inelastic behaviors of reinforced concrete shear wall-frame structures under monotonic and cyclic loading.

The purpose of this paper is to verify a validity and an applicability of the proposed analytical model through several numerical applications.
First of all, tensile bond specimen of Fig.1 are analyzed by both the proposed and the linkage model, and then bond behaviors are compared with experimental ones and a stress transfer process due to cracking is investigated.

Secondly, concrete panels contained by a square grid of equal reinforcing bars ,which were tested under uniaxial tension, are analyzed by the proposed model, and an influence of inelastic effects; bond, aggregate interlock and dowel action, on several behaviors is studied.

Finally, in order to understand monotonic and cyclic behaviors of reinforced concrete shear walls analytically, two different types of shear walls are analyzed by the proposed model. Specimen of the first type, Fig.15, is the reinforced concrete shear wall-frame structure with one bay and three stories under the combined stresses of axial force, bending moment and shear force, and solutions under monotonic horizontal loading such as load-deflection curve, crack propagation and stress transfer are compared with experimental results. Specimens of the second type, Fig.26, are reinforced concrete shear wall-frame structures tested under concentrated loading of simply supported beam's type, and cyclic behaviors and an influence of inelastic effects on them are studied.

2. TENSILE BOND SPECIMEN

It is an important subject to make an analytical model being capable of representing bond behaviors between reinforcing bar and concrete accurately, and to incorporate it into an analytical procedure in clarifying static hysteresis of reinforced concrete structures. In order to verify a validity of the bond model proposed by the authors in the reference[1], numerical solutions on the tensile bond specimens tested by Morita[2], as indicated in Fig.1, are compared with experimental results. Furthermore, finite element solution by the linkage element proposed by Ngo and Scordelis[3] which idealizes the bond stress (u) - relative slip(S) relation proposed by Morita et al.[4] as shown in Fig.2 are also presented with a view to investigating stress transfer process due to cracking minutely.

The linkage element is a spring element being composed of the bi-directional springs as shown in Fig.3 which has spring stiffnesses $K_{\bar{X}}$ and $K_{\bar{Y}}$ in the orthogonal directions $\bar{X},\bar{Y}$ and letting an angle between the local coordinates $\bar{X},\bar{Y}$ and the global coordinates X,Y be ${}_s\theta$, then the relation between the incremental displacements $\Delta\{\delta\}= \{\Delta\delta_1, \Delta\delta_2, \Delta\delta_3, \Delta\delta_4\}$ and the incremental nodal forces $\Delta p\{\bar{p}\}= \Delta p\{ \bar{p}_1, \bar{p}_2, \bar{p}_3, \bar{p}_4\}$ in the global coordinate system is given as follows,

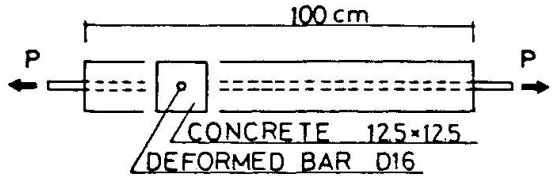

Fig.1 Tensile Bond Specimen

$$\Delta p\{\bar{p}\} = [k]\Delta\{\delta\}$$

in which

$$[k]=\begin{pmatrix} K_{\bar{x}}\cos^2_s\theta+K_{\bar{y}}\sin^2_s\theta & (K_{\bar{x}}-K_{\bar{y}})\cos_s\theta\sin_s\theta & -K_{\bar{x}}\cos^2_s\theta-K_{\bar{y}}\sin^2_s\theta & (K_{\bar{y}}-K_{\bar{x}})\sin_s\theta\cos_s\theta \\ & K_{\bar{x}}\sin^2_s\theta+K_{\bar{y}}\cos^2_s\theta & (K_{\bar{y}}-K_{\bar{x}})\sin_s\theta\cos_s\theta & -K_{\bar{x}}\sin^2_s\theta-K_{\bar{y}}\cos^2_s\theta \\ & & K_{\bar{x}}\cos^2_s\theta+K_{\bar{y}}\sin^2_s\theta & (K_{\bar{x}}-K_{\bar{y}})\sin_s\theta\cos_s\theta \\ \text{SYM.} & & & K_{\bar{x}}\sin^2_s\theta+K_{\bar{y}}\cos^2_s\theta \end{pmatrix}$$

and $K_{\bar{x}} = K_i \pi D l_b$ with k=1, 2 and 3 , $\Delta u = K_i \Delta S$

The spring stiffness $K_{\bar{x}}$ parallel to reinforcing bar is calcualted by multiplying slopes K_1, K_2 and K_3 of bond stress-relative slip curve of Fig.2 by the artificial bond area over which one spring governs. On the other hand, since a physical meaning of stiffness $K_{\bar{y}}$ perpendicular to reinforcing bar is not obvious so far, it is set equal to zero value. Cracks are also idealized by the linkage element and the stiffnesses $K_{\bar{x}}$, $K_{\bar{y}}$ are set equal to big values before crack formation or after the closing of cracks, and they are set equal to zero values when cracks open.

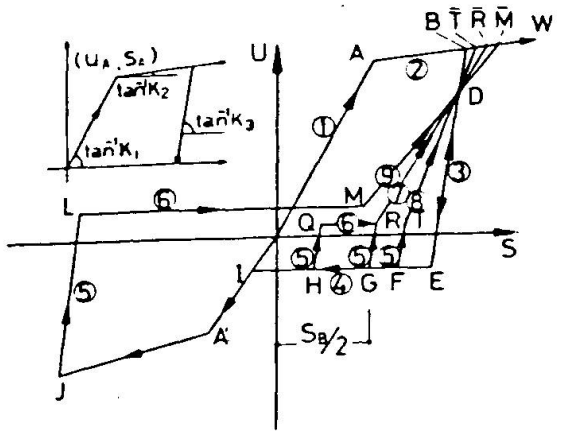

Fig.2 Cyclic Bond Stress-Relative Slip Relation

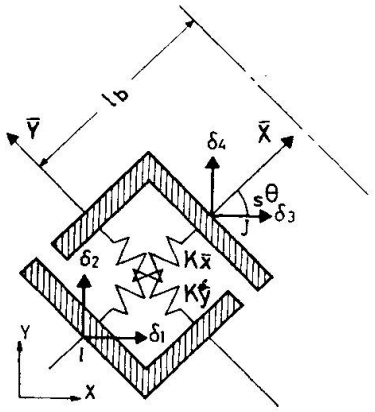

Fig.3 Linkage Element

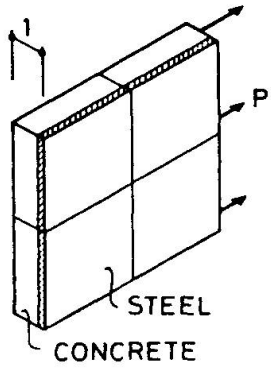

Fig.4 Finite Element Idealization by Proposed Model

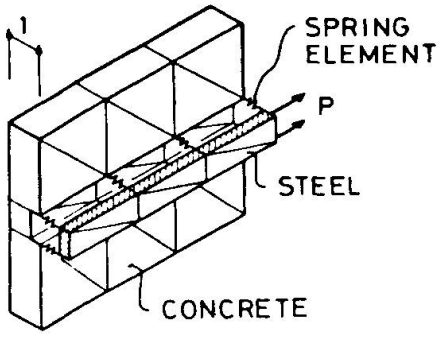

Fig.5 Finite Element Idealization by Linkage Model

Table 1. Material Properties of Bond Specimen

Material		Young's Modulus E (kg/cm^2)	Poisson's Ratio υ	Tensile Strength f_t (kg/cm^2)
Reinforcing Bar		2.0×10^6	0.3	———
Concrete	Specimen of Type 1 (Monotonic)	2.8×10^5	0.167	24.0
	Specimen of Type 2 (Cyclic)	2.8×10^5	0.167	21.5

Table 2. Characteristic Values for Linkage Model

Loading Direction	u_A (kg/cm^2)	S_A (cm)	K_1 (kg/cm^3)	K_2 (kg/cm^3)	K_3 (kg/cm^3)
Positive	46.875	0.00525	8929	687	17858
Negative	-46.875	-0.00525	8929	687	17858

The assigned finite elements are shown in " Figs.4 and 5 " respectively. " Tables 1 and 2" indicate material properties used in the analysis. " Fig.6" shows load-average strain curves for both the models on the tensile specimen under monotonic loading. " Fig.7" shows equivalent stress-average strain curves non-dimensionized by the cracking strength of concrete. " Fig.8" shows distributions of bond stresses and steel stresses at the loads of 4, 5 and 8 tons obtained by the linkage model.

It is found from Figs.7 and 8 that analytical results for both the models relatively agree with experimental ones and thus the assumptions made in the bond modelling may be reasonable. The reason why the initial stiffness of the proposed model is higher than the experimental one perhaps may be due to the assumption of perfect bond before cracking. The equivalent stresses of the linkage model suddenly increase against strains over about 0.0013 and this is considered to be attributable to the fact that the cracking positions are fixed to two sections on the basis of the experimental cracking pattern and thus internal cracks are not considered in the analysis.

Analyzing the process from results of Fig.8 in which the equivalent stress decreases with an increase of average strain, it can be seen that while bond stress changes with an increase in number of cracks as shown in the figure, concrete stress at the cracking parts is transfered to reinforcement and a resistance of concrete gradually deteriorates.

" Figs.9 and 10" show two cycles of load-average strain curves for both the models in which unloading was carried out at the strains of 0.0012 and 0.002. " Fig.11" shows the equivalent stress-average strain curve non-dimensionized by the cracking strength of concrete. The area of hysteresis loop for the proposed model is somewhat smaller than that of the experiment, but their correlation is satisfactory and particularly the slope of a line connecting a unloading point and a reloading point relatively agrees with the experimental one.

3. REINFORCED CONCRETE PANEL

In order to investigate a validity of the modelling of bond effect, aggregate

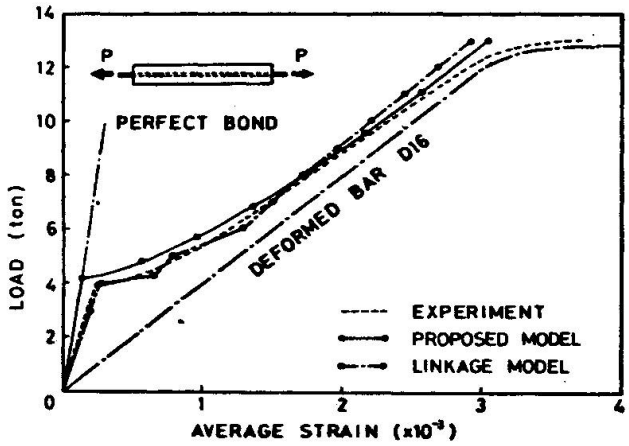

Fig.6 Load-Average Strain Curve under Monotonic Loading

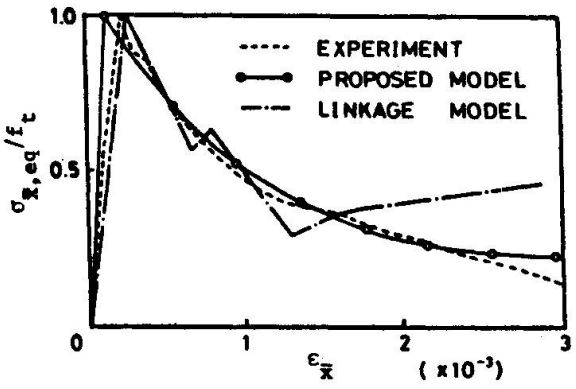

Fig.7 Non-Dimensionized Equivalent Stress-Average Strain Relation

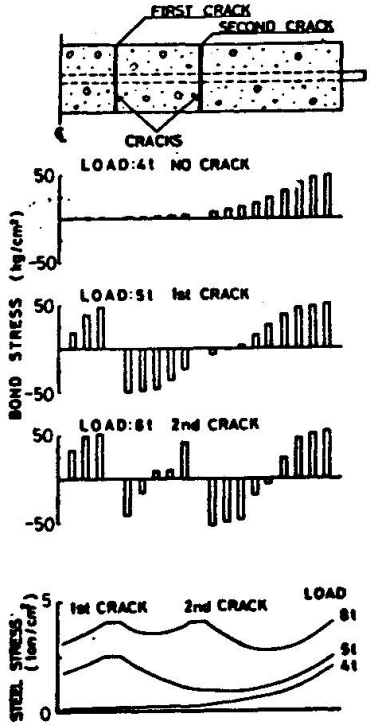

Fig.8 Distributions of Bond Stresses and Steel Stresses by Linkage Model

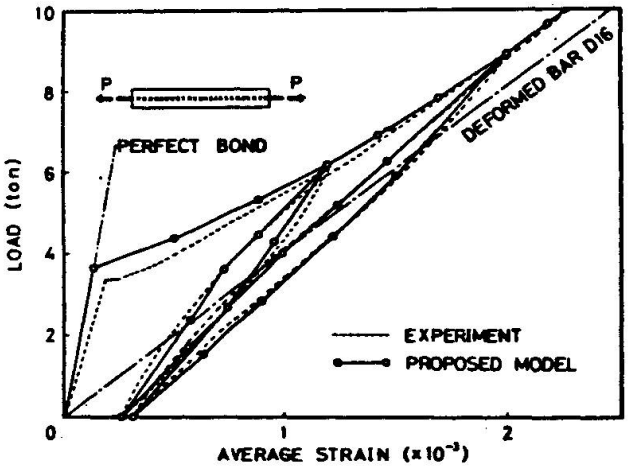

Fig.9 Load-Average Strain Curve by Proposed Model under Cyclic Loading

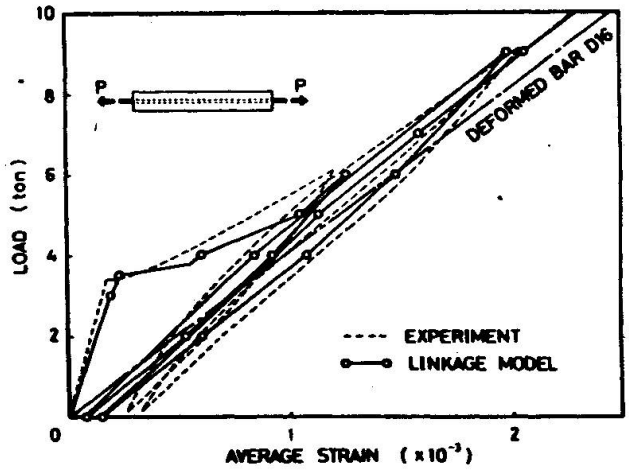

Fig.10 Load-Average Strain Curve by Linkage Model

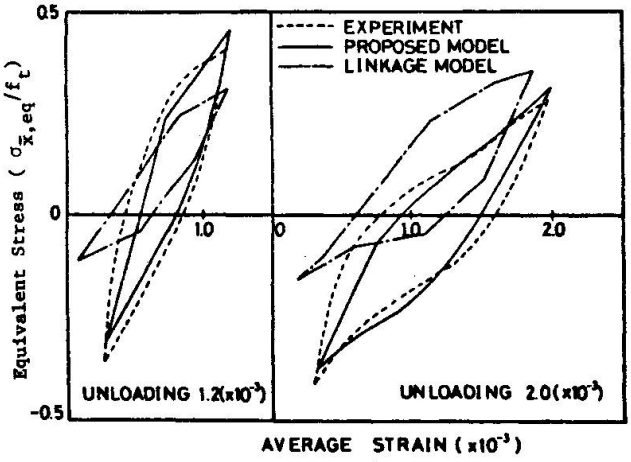

Fig.11 Non-Dimensionized Equivalent Stress-Average Strain Curve

interlock and dowel action formulated in the reference[1], numerical results by the proposed model are compared with Peter's experimental results[5] on reinforced concrete panels tested under uniaxial tension and theoretical values by Cervenka et al [6]. The test specimens were square concrete panels subjected to uniaxial tension as shown in " Fig.12" and they contained a square grid of equal reinforcing bars. The variable factor of this experiment is an angle θ between the reinforcing direction and the loading direction, and here five specimens with $\theta = 0^0$, 10^0, 20^0, 30^0 and 40^0 are comparatively studied. " Table 3" indicates material properties and note that in order to obtain predicting cracking loads consistent with experimental ones, tensile strengthes linearly interpolated from principal stresses by the elastic analysis are used in the analysis instead of those determined from the material test.

"Figs.13(a), (b), (c), (d) and (e)" compare load-extension curves predicted by the proposed model with those observed by the experiment and they also contain theoretical values by Cervenka et al. which do not take bond, aggregate interlock and dowel action into consideration. The numerical result of the proposed model for $\theta = 10^0$ (Type 2) which considers bond but no aggregate interlock and dowel action is given in Fig.13 (b).

Numerical results by the proposed model relatively agree with experimental ones except the case of $\theta = 40^0$ and it may be known that a effect of bond, aggregate interlock and dowel action on stiffness after crack formation is serious.
It is seen from Fig.13(b) that an influence of aggregate interlock and dowel action on predicted loads is from 3 to 8 percents and thus it is relatively

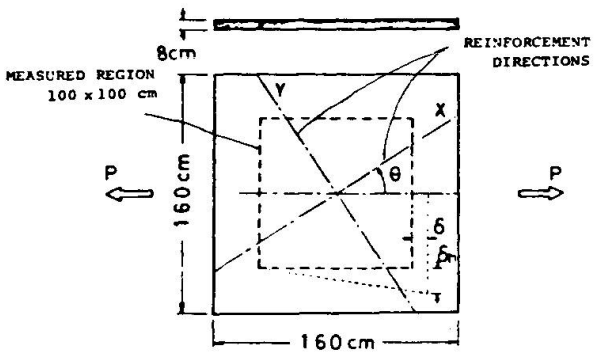

Fig.12 Reinforced Concrete Panel subjected to Uniaxial Tension

Table 3. Material Properties of Reinforced Concrete Panels

Specimen	Reinforcement (ϕ 8)					Concrete		
	p_x (%)	p_y (%)	$_sE$ (kg/cm^2)	$_sE_{sh}$ (kg/cm^2)	θ	f_c (kg/cm^3)	f_c^* (kg/cm^2)	E(kg/cm^2)
S 2r 0	0.6625	0.6625	2.08 x 10^6	6.6 x 10^4	0	18.5	14.56	2.5 x 10^5
S 2r10	0.6625	0.6625	2.08 x 10^6	6.6 x 10^4	10	23.4	14.93	2.5 x 10^5
S 2r20	0.6625	0.6625	2.08 x 10^6	6.6 x 10^4	20	23.1	12.78	2.5 x 10^5
S 2r30	0.6625	0.6625	2.08 x 10^6	6.6 x 10^4	30	20.9	15.24	2.5 x 10^5
S 2r40	0.6625	0.6625	2.08 x 10^6	6.6 x 10^4	40	27.6	15.70	2.5 x 10^5

* the tensile strength used in the analysis

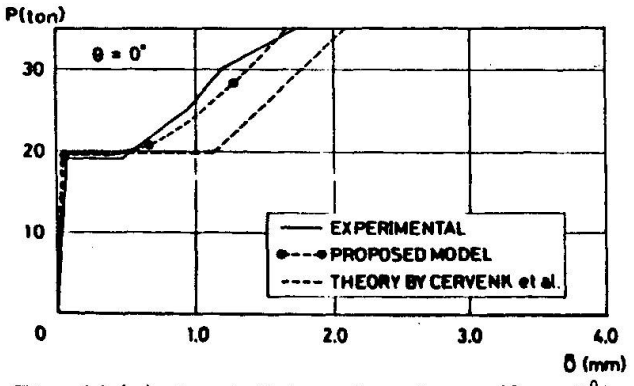

Fig.13(a) Load-Extension Curve($\theta = 0^0$)

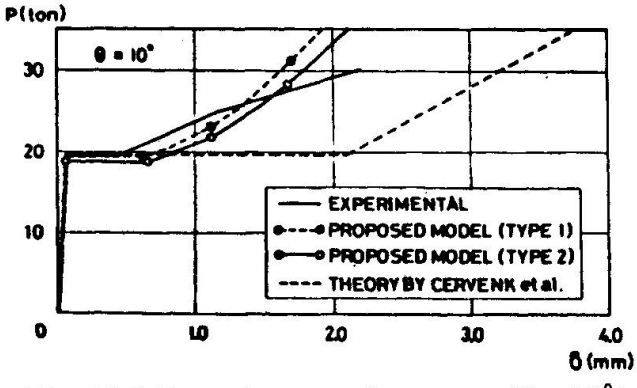

Fig.13(b) Load-Extension Curve($\theta = 10^0$)

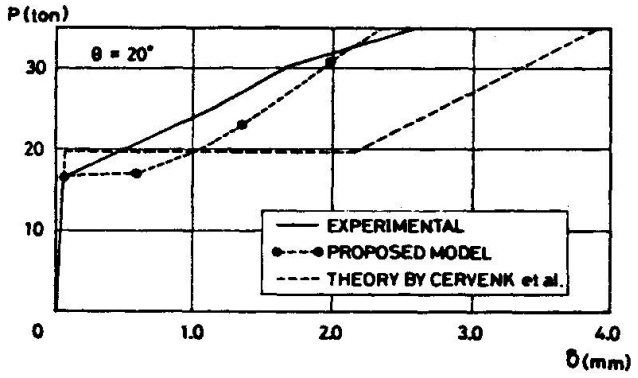

Fig.13(c) Load-Extension Curve($\theta = 20^0$)

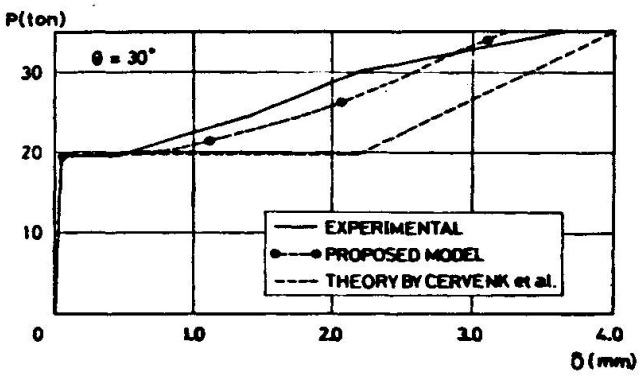

Fig.13(d) Load-Extension Curve($\theta = 30^0$)

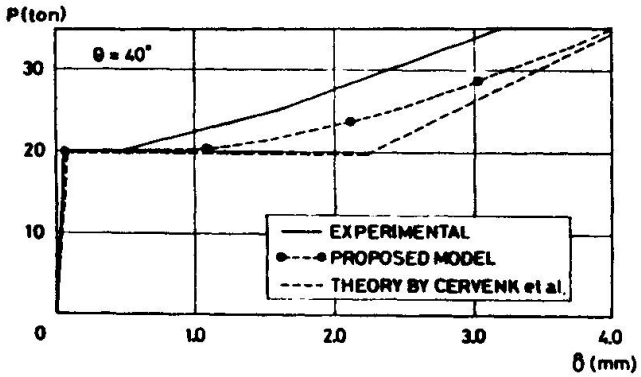

Fig.13(e) Load-Extension Curve($\theta = 40^0$)

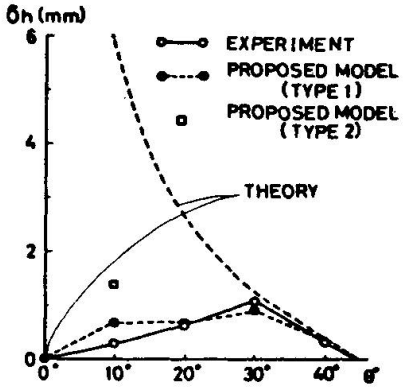

Fig.14 Effect of Reinforcing Direction on Transverse Displacement

small in the case of this specimen and loading condition.

In the next place, " Fig.14" shows plots of transverse displacements δ_h at the load p = 35 tons ($\theta = 0^0$, 20^0, 30^0 and 40^0) and at p = 30 tons ($\theta = 10^0$) against the reinforcing direction θ along with theoretical values by Cervenka et al. , where δ_h means the shear displacement of Fig.12 induced by uniaxial tension. Results of the proposed model and the experiment give a good correlation and as it is seen from theoretical values, an analysis which ignores bond, aggregate interlock and dowel action leads to a big discrepancy in results for specimens with reinforcing angles less than 30^0.
It is found that a contribution of aggregate interlock and dowel action to shear displacements is big to be about 50 percents unlike the contribution of these to predicted loads.

4. REINFORCED CONCRETE SHEAR WALL - FRAME STRUCTURE

4.1 Behavior under Monotonic Loading

In order to investigate behaviors of reinforced concrete shear wall-frame structures, the authors et al.[7] conducted a large number of cycles of alternative loading tests on eighteen reinforced concrete shear wall-frame specimens of about one-fifth of actual size with I-shaped cross section of three stories and one bay

which simulated lower portions of buildings.
" Fig.15" shows the detail of bar arrangement of specimen, that is, one among eighteen specimens and " Table 4" indicates structural dimensions of specimen, and here analytical results such as load-deflection curve, crack propagation, stress transfer, etc. are compared with experimental ones minutely.
The cantilever beam system for loading was adopted as shown in " Fig.16" and the foundation part of specimen was fixed to the test floor by using six prestressed concrete steel bars and introducing 25 tons of prestress a bar. Concentrated horizontal loads were applied to the center line of uppermost story's beam from either the left or the right hand side with an application of constant vertical load of 13.5 tons to tops of surrounding columns equally.

The failure progression of this specimen was as follows(see Fig.22). Shear cracks at the corner of wall, flexural cracks at the bottom of column in the tension side and major shear cracks at the center of wall in the first story occured in order respectively, and thereafter minor shear cracks occured in the wall panels of each story. Main reinforcement at the bottom of column in the tension side yielded in the member rotation angle $R = 4.32 \times 10^{-3}$ rad.(horizontal deflection $\delta = 7.45$mm). The maximum loading capacity was attained in the first cycle of $R = 10.0 \times 10^{-3}$ rad.($\delta = 17.25$mm) and diagonal cracks of column in the compression side was observed on the way to the subsequent cycles of $R = 10.0 \times 10^{-3}$ rad. and thereafter the splitting along main reinforcement of column in the compression side and the protrusion of cover concrete followed by the buckling of main reinforcement were observed on the way to $R = 20.0 \times 10^{-3}$ rad. ($\delta = 34.5$ mm) and then the specimen reduced its strength largely along with the progression of concrete crushing at the corner of wall in $R = 14.7 \times 10^{-3}$ rad. ($\delta = 25.36$ mm).

"Tables 4 and 5" indicate material properties obtained from the material test of reinforcing bar and concrete, and "Table 6" indicates material properties adopted in the analysis. The specimen is seperated into 93 super elements, that is, 372 finite elements as shown in "Fig.17". The specimen was analyzed by the initial stress approach. First equal axial loads of 3.375 tons were vertically applied to nodes of 1, 2, 7 and 8 respectively and then 23 incremental displacements up to $R = 15.2 \times 10^{-3}$ rad.($\delta = 26.0$ mm) were given in the horizontal direction of the node 1, and note that at the same time relatively big axial loads were vertically applied to upper nodes of foundation elements in

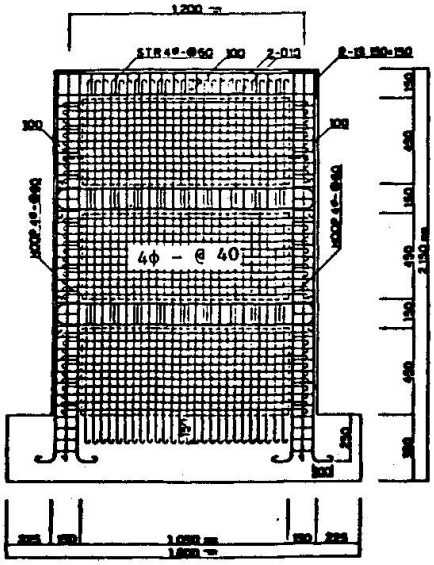

Fig.15 Detail of Reinforced Concrete Shear Wall Specimen

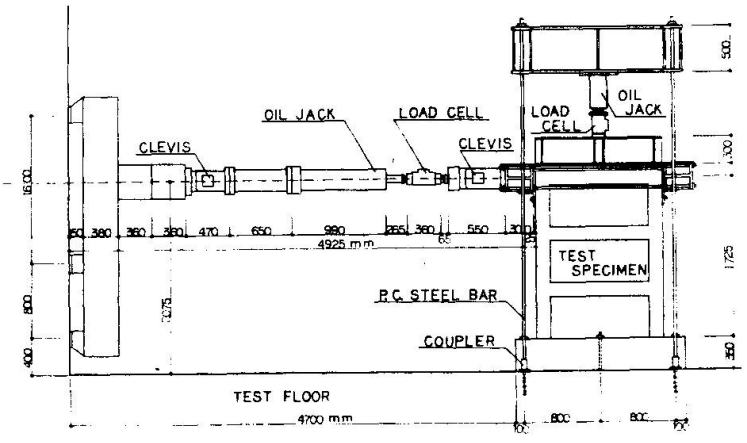

Fig.16 Loading Setup

order to simulate a settlement of foundation. Von-Mises's yield criterion was used for plastification of concrete in compression in this analysis.

"Fig.18" shows load-deflection curve of the proposed model(Type 1) calculated by considering all inelastic effects and that(Type 2) by neglecting bond, aggregate interlock and dowel action along with the experimental one.
Both analytical results fairely coincide with the experimental one, but predicted loads of Type 2 give a some what smaller estimation than the experiment after flexural yielding.

"Fig.19" shows plots of ratios of differences between predicted loads of Type 1 and Type 2 at the same deflection levels to predicted loads of Type 1 against horizontal deflections, and these quantities mean a contribution of bond, aggregate interlock and dowel action to the load-carrying capacity.
An influence of these inelastic effects is relatively big to be about 8-18 percents before the yielding loads(P = 20.85 tons) and on the other hand it is small to be about 2-10 percents after the yielding load though there are some scatters.

"Fig.20" shows the principal stress distribution of Type 1 at the elastic stage (P = 4.49 tons and δ = 0.45 mm). The compression field extending from the loading point toward the bottom of column in the compression side is formed and it is considered that the principal stress distribution at the elastic stage roughly determines crack formation and angles of concrete.

"Fig.21" shows the predicted cracking pattern of Type 1 at the load P = 27.26 tons the horizontal deflection δ = 24.0 mm, where the single line indicates the cracked element and its inclination indicates the crack angle, the shaded portion indicates the strain-softening element, and the black solid indicates the crushing element. "Fig.22" shows the final cracking pattern observed by the experiment. The cracking pattern predicted by the analysis fairely agrees with the experimental one and it is understood that the crushing of concrete at the corner of wall and at the bottom of column in the compression side in the first story is a direct cause of a failure.

"Figs.23(a) and (b)" show shear stress distributions of Type 1 along several horizontal cross sections of specimen at P = 4.49 tons,δ = 0.45 mm and at P = 27.26 tons, δ = 24.0 mm respectively. The shear stress distribution of Fig. 23(a) except that for the third story is close to that of I-shaped cross section being assumed in the conventional elastic theory and therefore shear stresses near the center of wall panel are maximum. On the other hand, as it is known from Fig.21, noting that shear stresses near the bottom of column in the compression side at the first story are zero since the crushing has been occured in the corresponding elements, shear stresses near the diagonal line connecting the loading point and the bottom of column in the compression side at the first story are maximum.

"Fig.24" shows the load-strain curve of Type 1 for the main reinforcement at the bottom of column in the tension side. The analysis gives a little bit higher yielding load than that of the experiment, but it is considered that this prediction is sufficiently accurate in spite of the assumption that the area of reinforcement distributes uniformly within any concrete element.

"Figs.25(a) and (b)" show a comparison between crack widths predicted by the analysis of Type 1 and measured crack widths at the center of wall panels in the first and second story. Measured widths are wider than predicted ones, but here it should be noted that widths of the experiment were measured on the concrete surface and on the other hand widths of the analysis were evaluated on the

Table 4. Structural Dimensions of Specimen

Shear Span Ratio	Column Section (cm x cm)	Beam Section (cm x cm)	Wall Thickness (cm)	Main Bar in Column (p %)	Main Bar in Beam (p %)	Hoop in Column (p %)	Wall Reinforcement (p_x %)	(p_y %)
1.28	15 x 15	15 x 15	4.5	8 - D10 (2.53)	4 - D10 (1.46)	4φ - a 60 (0.28)	4φ - a 40 (0.72)	4φ - a 40 (0.72)

Table 5. Material Properties of Reinforcement

Steel	$_sA$ (cm^2)	$_s\sigma_y$ (kg/cm^2)	$_s\varepsilon_y$ ($\times 10^{-6}$)	$_s\sigma_B$ (kg/cm^2)	$_sE$ ($\times 10^6$ kg/cm^2)
D10	0.71	3761	1896	5279	1.96
4φ	0.127	5398	4559	5784	2.11

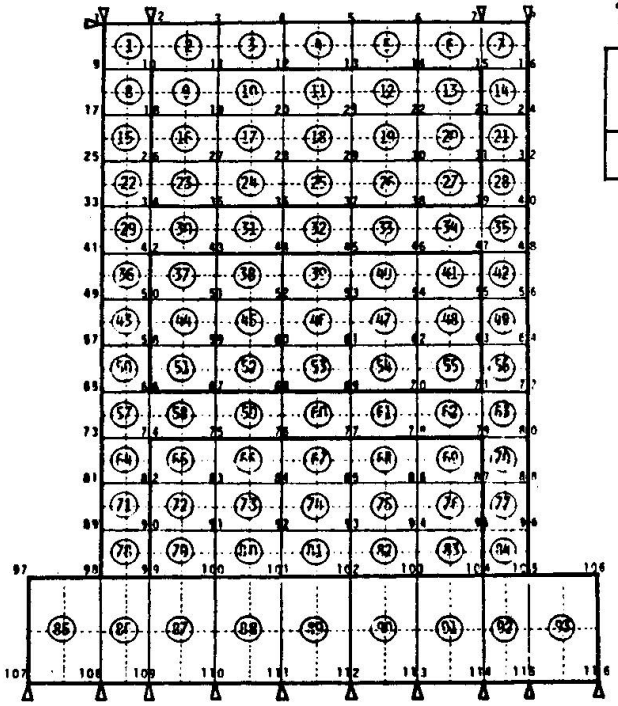

Fig.17 Finite Element Discretization

Table 6. Material Properties of Concrete

E (kg/cm^2)	υ	σ_B (kg/cm^2)	ε_B (kg/cm^2)	f_t (kg/cm^2)
2.25×10^5	0.196	226	2240×10^{-6}	27.9

σ_B : the compressive strength

ε_B : the strain at the compressive strength

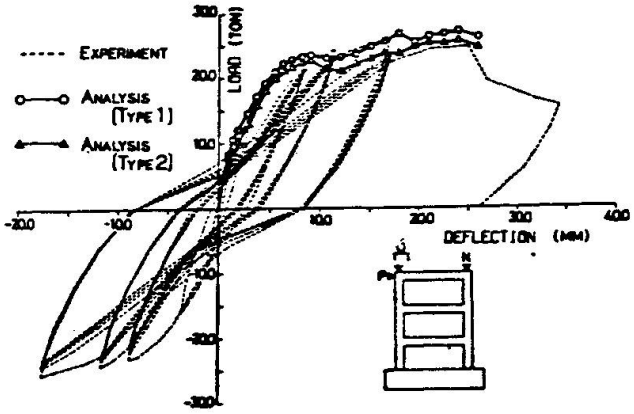

Fig.18 Horizontal Load-Deflection Curve

Table 7. Material Properties used in the Analysis

Material		Young's Modulus (kg/cm^2)	Yield Stress (kg/cm^2)	Poisson's Ratio υ
Concrete		$E = 2.25 \times 10^5$	$\sigma_{y1} = 162$	0.196
		$E_{t1} = 0.323 \times 10^5$	$\sigma_{y2} = 226$	
		$E_{t2} = -0.613 \times 10^5$	———	
Steel	D10	$_sE = 1.96 \times 10^6$	$\sigma_y = 3761$	———
		$_sE_{sh} = 1.49 \times 10^4$	———	
	4φ	$_sE = 2.11 \times 10^6$	$\sigma_y = 5398$	———
		$_sE_{sh} = 1.99 \times 10^6$	———	

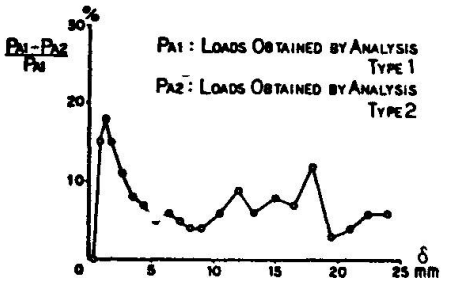

Fig.19 Contribution of Bond, Aggregate Interlock and Dowel Action to Loads

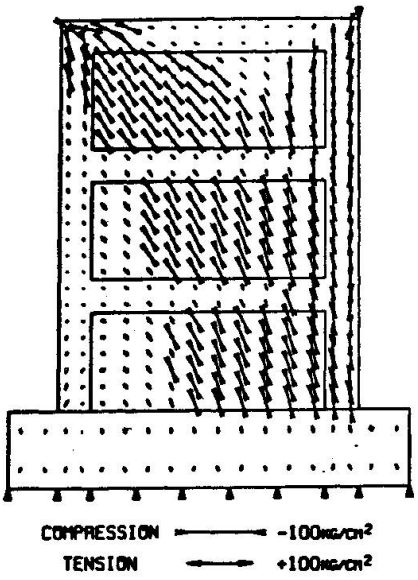

Fig.20 Principal Stress Distribution at P=4.49(t)

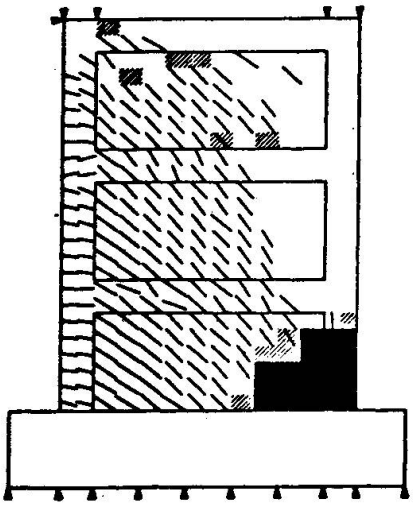

Fig.21 Predicted Cracking Pattern at P=27.26 (t)

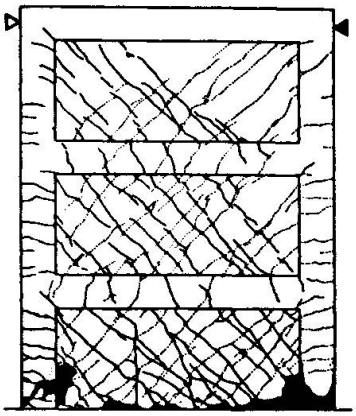

Fig.22 Final Cracking Pattern of Experiment

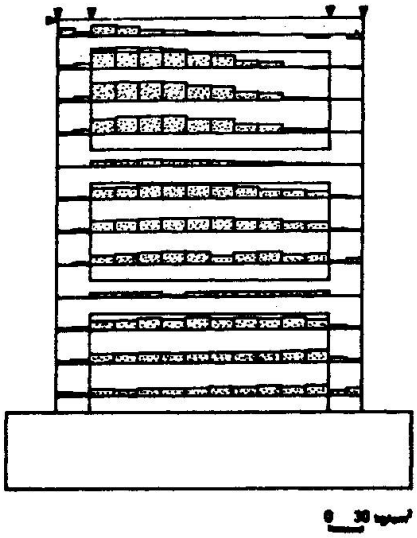

Fig.23(a) Shear Stress Distribution at P = 4.49 (t)

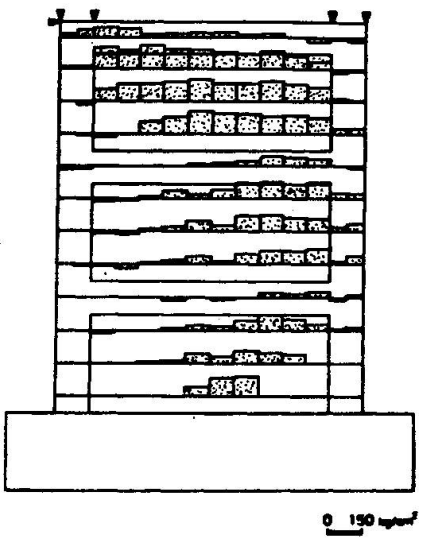

Fig.23(b) Shear Stress Distribution at P = 27.26 (t)

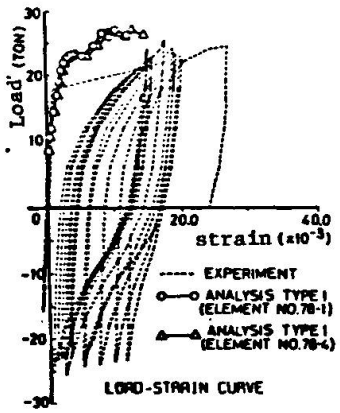

Fig.24 Load-Strain curve for Main Reinforcement

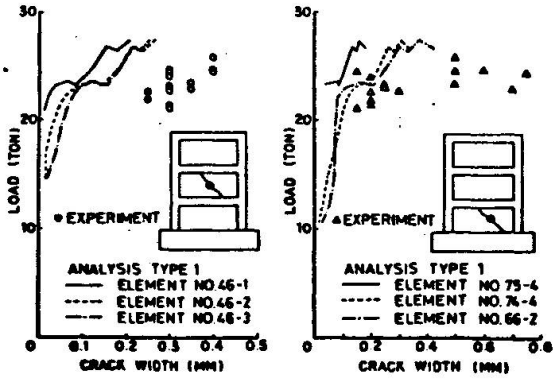

Figs.25(a),(b) Load-Crack Width Relation

exposed surface of reinforcement. Judging from the experimental result[8] on tensile bond specimen in which ratios of widths on the exposed surface of reinforcement to those on the concrete surface are from 75 to 80 percents in the case of smooth round bars, it is thought that predicted crack widths are nearly satisfactory estimation.

4.2 Behaviors under Cyclic Loading

In order to examine a validity of the proposed model, an analysis is conducted on two reinforced concrete shear wall-frame specimens[9] with the same configurations and details, where the detail of specimen is shown in "Fig.26", but different wall thicknesses, where the thickness of Type 1 is 7.8 cm and that of Type 2 is 7.5 cm, and loading excursions, and a comparison with experimental results is made. The specimen was composed of two symmetrical structural systems and they were tested as a simply supported beam.
"Tables 7 and 8" indicate material properties of steel and concrete.

The specimen was seperated into 30 super elements as shown in "Fig.27" and it was analyzed by the self-correcting approach. Von-Mises's yield criterion was adopted for plastification of concrete in compression in this analysis.

"Fig.28(a)" shows the load-deflection curve for the specimen of Type 1 in which unloading was done at the deflection of about 1.0 mm and then reloading was done from zero-load level. "Fig.28(b)" shows the load-deflection curve for the specimen of Type 1 without a consideration of bond effect.
Analytical results by Schnobrich et al.[10] and Darwin et al.[11] are also included in Fig.28(a), where the former considers no bond effect but aggregate interlock and dowel action as one-quarter of the elastic shear stiffness G for the cracked concrete and the latter does not consider bond effect, aggregate interlock and dowel action. The analytical result by the proposed model gives a somewhat smaller area of hysteresis loop than that of the experiment, but it gives a fairely good agreement with the experiment as a whole.

If bond effect is not considered, it is found that the analysis not only underestimates loads in the region of relatively small deflections, but also results in a big discrepancy in cyclic behaviors.
Furthermore, it is possible to correspond the anatytical load-deflection curve in the early stage to the experimental one by assuming appropriate constant values as the shear stiffness after crack formation, but such assumption leads

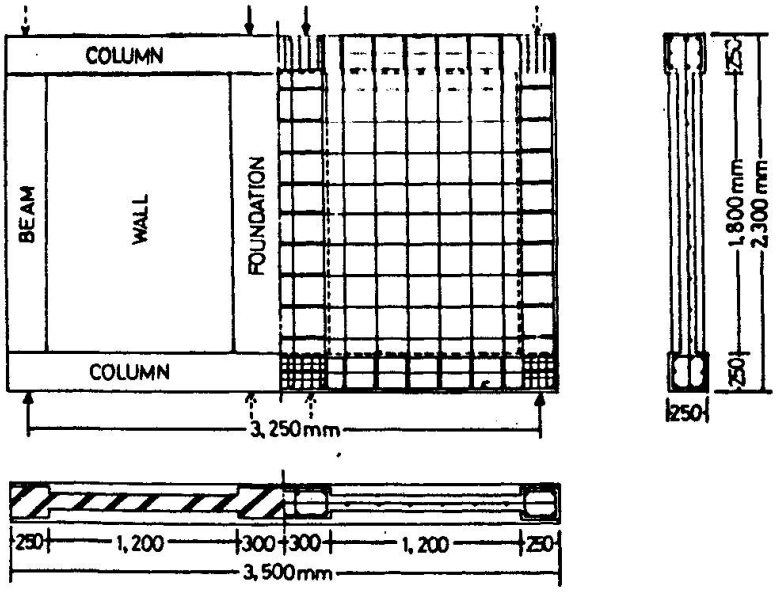

Fig.26 Detail of Reinforced Concrete Shear Wall Specimen

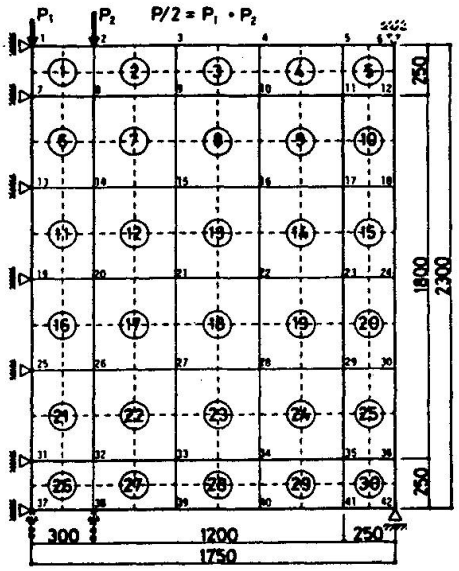

Fig.27 Finite Element Discretization

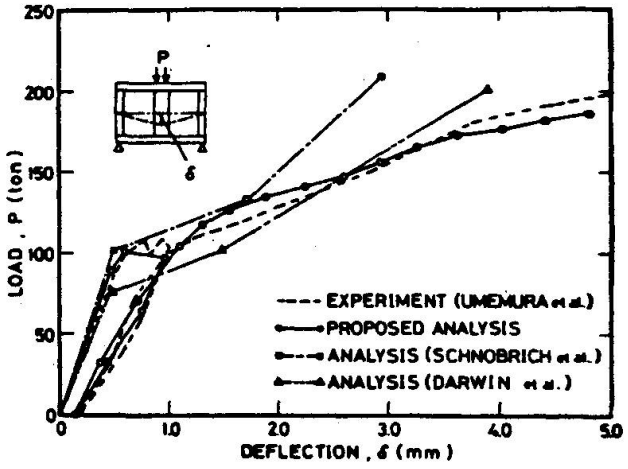

Fig.28(a) Load-Deflection Curve for Specimen of Type 1

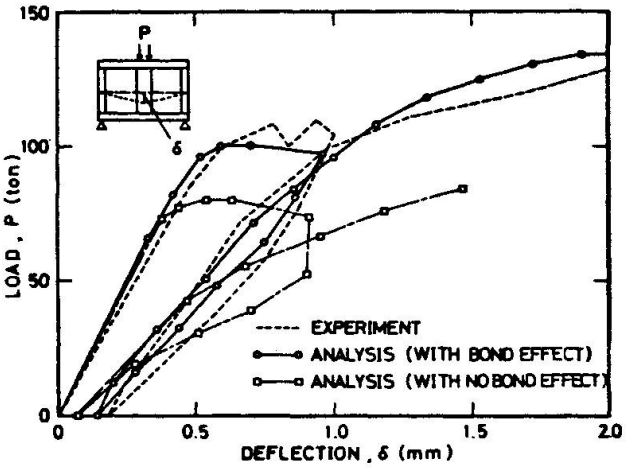

Fig.28(b) Load-Deflection Curve for Specimen of Type 1

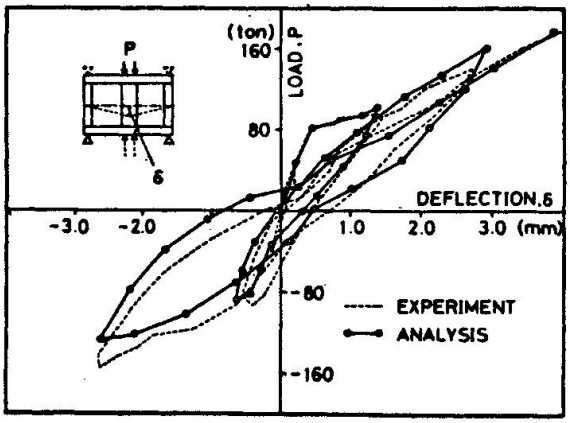

Fig.29 Load-Deflection Curve for Specimen of Type 2 under Alternative Cyclic Loading

to an overestimation of loads as deflections become larger.

"Fig.29" shows two cycles of load-deflection curve for the specimen of Type 2 in which unloading was conducted at the deflections of + 1.4 , - 0.6 , + 2.7 and - 2.6 mm respectively.
The analytical load-deflection relation has a tendency that a recovery of strength is late and deflections become larger in the negative loading cycles, but the configuration of hysteresis loop is similar to the experimental one and also the analytical result relatively agrees with the experimental one as a whole.

5. CONCLUSION

The following conclusions were obtained from an evaluation of the proposed model described in the reference[1] and a comparison between analytical results and experimental ones,

- It is necessary for pursuing hysteresis behaviors of reinforced concrete structures to consider bond effect and the proposed bond model is effective in

such a sense that its accuracy is high and an incorporation it into the analytical procedure is easy. However, the furtherdevelopment of bond model is required to consider the different type of bar surface(smooth round bar or deformed bar) and the effect of transverse pressure field as observed in wall panels on bond behaviors.

- Aggregate interlock and dowel action could be idealized as the equivalent shear stiffness depending upon static hysteresis by considering crack spacing and width. Although the effect of these inelastic effects on behaviors is different depending upon the type of structures and loading conditions, an influence of these effects on deflections,that is, shear displacements is greater than that of these on loads and particularly the new model of aggregate interlock gives a reasonable result, for example as indicated in Fig.28(a).

- The predicted failure pattern nearly corresponds to that observed by the experiment.

- The analysis tends to underestimate crack widths and furthermore it is considered that the judgement of crack closing in the cyclic analysis is the remaining question.

- The incremental self-correcting approach is valuable to reduce the computational time and also gives satisfactory results. However, it must note that the effect of incremental size of load factor on behaviors is serious.

REFERENCE

1. N.Shirai and T.Sato,"Inelastic Analysis of Reinforced Concrete Shear Wall Structures : Material Modelling of Reinforced Concrete," IABSE Colloquium, Delft, 1981.
2. S.Morita et al.,"Bond-Slip Relationship under Repeated Loading," Transactions of Architectural Institute of Japan, No.229, 1975 (in Japanese).
3. Ngo,D., and A.C.Scordelis,"Finite Element Analysis of Reinforced Concrete Beams," Journal of ACI, Vol.64, No.3, March 1967.
4. S.Morita,"Study on Bond Effect of Reinforced Concrete Members by Tensile Tests ," The Annual Report of Cement Engineering, Vol.XVII, 1963 (in Japanese).
5. Peter,J.,"Zur Bewehrung von Scheiben und Schalen für Hauptspannungen schiefwinklig zur Bewehrungsrichtung," Dr.-Ing. Dissertation, T.H. Stuttgart, 1964.
6. V.Cervenka and K.H.Gerstle,"Inelastic Analysis of Reinforced Concrete Panels, Part I : Theory," IABSE Publications, Vol.31-II, 1971.
7. T.Sato, A.Ono, H.Adachi, N.Shirai and M.Nakanishi,"Experimental Study on Elast-Plastic Behavior of Reinforced Concrete Shear Wall Structures," Journal of the Research Institute of Science and Technology, Nihon University, No.53, July 1980 (in Japanese).
8. Y.Goto et al.,"Investigation on Tension Cracks in Reinforced Concrete Member : An Experiment by Tensile Bond Specimen," The 2nd Symposium on Deformed Bars , Concrete Library, No.14, 1965 (in Japanese).
9. H.Umemura et al.,"Studies on Reinforced Concrete Shear Wall and Framed Masonry Shear Walls," Research Report, University of Tokyo, 1964.
10. W.C.Schnobrich et al.,"A Numerical Procedure for the Determination of the Behavior of Shear Wall Frame System," Journal of ACI, 1973.
11. D.Darwin et al.,"Inelastic Model for Cyclic Biaxial Loading of Reinforced Concrete," Civil Engineering Studies, SRS-No.409, University of Illinois, 1974.